BMC Oral Health

RESEARCH

Open Access

EDA1 variants inhibit the odontogenic differentiation and proliferation of human dental pulp stem cells

Yulin Ding[1,2†], Genqi Lu[1,3†], Ya Zhao[1], Yi Zhang[4], Jing Zhang[1,5], Jingle Ma[6], Yunyun Yuan[1], Boyu Liu[1], Wei Liu[7*] and Wenjing Shen[6*]

Abstract

Background Variants of Ectodysplasin A1 (EDA1) regulate the proliferation, migration, and odontogenic differentiation of human dental pulp stem cells (hDPSCs). Further study of these variants could reveal the mechanism by which EDA1 induces tooth development.

Methods The following groups of hDPSCs were studied: those expressing wild-type (Wt) *EDA1*, those expressing *EDA1* non-syndromic tooth agenesis (NSTA) variants (NSTA-A259E, NSTA-S374R), those expressing a syndrome type (STA) variant of *EDA1* (STA-H252L), and those transformed with the empty vector (NC, negative control). hDPSCs proliferation was assessed using Cell Counting kit 8 assays. Flow cytometry was employed to assess hDPSCs cell cycle distribution. Transwell and wound-healing assays were employed to assess hDPSCs migration. hDPSCs mineralization was induced using odontogenic differentiation medium. RNA sequencing of the various hDPSCs groups was carried out to identify enriched pathways and hub genes. Hub gene expression was confirmed using quantitative realtime reverse transcription PCR (qRT-PCR).

Results Wt-*EDA1* promoted hDPSCs proliferation and G0/G1 to S transition significantly compared with the NSTA-*EDA1* and STA-*EDA1* groups ($p < 0.01$). The NSTA-*EDA1* and STA-*EDA1* groups did not show significant differences between them ($p > 0.05$). Relative to that in the NSTA-*EDA1* and STA-*EDA1* groups, Wt-*EDA1* enhanced hDPSCs migration ($p < 0.01$). According to alkaline phosphatase and Alizarin Red staining, compared to the Wt-*EDA1* group, hDPSCs odontogenic differentiation was inhibited and proliferation was ablated in the NSTA-*EDA1* and STA-*EDA1* groups ($p < 0.01$). RNA sequencing showed enrichment of the MAPK signaling and osteoclast differentiation pathways, identifying *FOS* and *JUN* as differentially expressed hub genes. qRT-PCR demonstrated that, unlike the Wt-*EDA1* group, the *EDA1* variant groups could not promote *FOS* mRNA expression.

Conclusions In hDPSCs, *EDA1* variants could not promote *FOS* expression, which inhibited hDPSCs odontogenic differentiation and ablated their proliferation.

†Yulin Ding and Genqi Lu contributed equally to this work.

*Correspondence:
Wei Liu
liuweihebmu@hebmu.edu.cn
Wenjing Shen
wenjingshen2020@hebmu.edu.cn

Full list of author information is available at the end of the article

Keywords Ectodysplasin A1, Proliferation, Migration, Odontogenic differentiation, Human pulp stem cells, c-FOS

Background

A lack of teeth caused by failure of development is termed tooth agenesis (TA), comprising one of the most frequently encountered developmental malformations, with significant aesthetic, masticatory, and psychological consequences. More than 300 genes are involved in various phases of tooth development. During the development of the embryo, underlying mesenchyme–surface epithelial cell interactions can be disrupted by mutations in these genes, resulting in the abnormal initiation, formation, and differentiation of skin appendages. Ectodysplasin A (EDA) signaling pathways have vital functions in embryonic ectodermal development [1–2].

The *EDA* gene, located on chromosome Xq12-13.1, encodes a tumor necrosis factor (TNF) superfamily member. In 1996, Kere et al. identified that the total length of the human *EDA* is 425 kb, consisting of 12 exons, and encoding EDA1 with 391 amino acids. *EDA* is differentially expressed in specific regions and stages of tooth development, and its transcriptional activity is regulated by activating the EDA-nuclear factor kappa B (NF-κB) signaling pathway [3]. Mues and Shen demonstrated that *EDA1* variants in non-syndromic tooth agenesis (NSTA) have a reduced binding ability for their specific receptor [Ectodysplasin A Receptor (EDAR)], whereas syndromic mutations in *EDA1* are associated with syndromic tooth agenesis (STA) and have completely lost this binding ability [4]. This results in a reduction or loss of the transcriptional activity of the downstream signaling factor, NF-κB [5], consequently decreasing the proliferation capacity of odontogenic cells. However, overexpression of EDA1 can promote cell proliferation in the dental lamina, facilitate the development of additional substrates, and enhance the transcriptional activity of NF-κB [6].

In human embryos, EDA1 is detected in ectodermal tissues and the developing neuroectoderm, thymus, and bone. Compared with a WT type skull, a Tabby skull (EDA deficiency) has significantly reduced bone marrow space and thicker cortical bone. Similar phenomena have been observed in the skull and jawbone of patients with Hypohidrotic ectodermal dysplasia (HED). The postnatal regulation of bone formation/resorption requires EDA, and research has found that this might be related to reduced expression of coenzymes associated with osteoclastogenesis, leading to postnatal bone homeostasis disorders [6–8]. This suggested that the differentiation of osteoblasts is preceded by EDA/EDAR signaling events. During tooth embryo development in Tabby mice, the tooth bud develops abnormally, becoming smaller in size, the number of teeth decreases after birth, and the number of tooth cusps is reduced, leading to undersized teeth [1]. Researchers analyzed the cDNA microarray expression profile of mouse skin, comparing wild-type mice, *EDA* deficient (Tabby) mice, and adult Tabby mice supplemented with the EDA-A1 subtype. The study revealed that the NEMO/ NF-κB pathway was down-regulated in the skin of Tabby mice. Additionally, the down-regulation of the JNK/c-jun/c-fos pathway and its target genes was even more pronounced [9]. Meanwhile, mesenchymal stem cells treated with iRoot SP were found to activate the NF-κB and MAPK signaling pathways, promoting osteogenic and odontogenic differentiation [10]. These findings suggest that the development of ectodermal organs relies heavily on the NF-κB and MAPK signaling pathways. According to reports, symptoms such as changes in tooth size and bovine dental disease can be observed in patients with HED, suggesting that EDA1 regulates the occurrence and development of teeth, and determines the fate of teeth.

Previous research revealed that NF-κB mostly mediates the effects of EDA1/EDAR signaling [11–12], although exactly how EDA1 regulates ectoderm development remains under investigation. Thus, the specific mechanism by which EDA1 regulates how dental stem cells develop into teeth requires further study. Our study utilized the characteristics of hDPSCs to investigate the effects of EDA1 on proliferation, migration, and mineralization during tooth development, as well as its regulatory mechanisms. This research provides new insights into the pathogenesis of congenital tooth loss.

Methods

EDA expression vectors

Professor Pascal Schneider (Department of Biochemistry, University of Lausanne, Switzerland) kindly donated mammalian vectors expressing secreted FLAG-tagged versions of Wt *EDA1* and *EDA1* with the HED-causing variant H252L. NSTAassociated variants of *EDA1* (A259E, S374R) were generously provided by Professor Hailan Feng (Department of Prosthodontics, Peking University School and Hospital of Stomatology, China) [5].

hDPSCs culture and transient plasmid transfection

The Oral Stem Cell Bank (Beijing Taisheng Biotechnology Co., LTD, Beijing, China) provided the hDSPCs. High-glucose Dulbecco's modified Eagle's medium (DMEM) with 10% fetal bovine serum was used to culture the hDSPCs at 37 ℃ in a 5% CO_2 atmosphere. After 12 h, the serum was removed. The hDPSCs were then seeded into 6-well cell culture plates at a density of 2×10^5 cells per well and cultured for 24 h. Plasmids of each group [Wt, STA-H252L, NSTA-A259E, NSTA-S374R, NC (negative

control)] were transfected into the cells using Lipofectamine 3000 (Invitrogen, Carlsbad, CA, USA).

Proliferation assays

Cell counting kit 8 (CCK8) assay

A CCK8 assay kit (Beyotime Biotechnology, Shanghai, China) was used to assess hDPSCs proliferation. 3 h after transfection, cells were seeded into a 96-well plate at a density of 6×10^3 per well. For each group, five parallel wells were set, with the control group receiving only 200 µl of medium. At 0, 12, 24, 48, 72, and 96 h, CCK8 reagents were added to the hDPSCs and incubated for 3 h at 37 ℃. A microplate reader (BioTek Instruments, Winooski, VT, USA) was then employed to measure the absorbance at 450 nm.

Flow cytometry

48 h after transfection, hDPSCs were digested with 0.25% trypsin solution and washed twice with precooled phosphate-buffered saline (PBS). The cells were then fixed with 70% ethanol at 4 ℃ for 24 h. The cells were suspended in 100 µl of PBS, mixed with 1 ml of propidium iodide (PI) solution, and stained at 4 ℃ for 30 min. Flow cytometry was then used to detect the cell data, and Multicycle AV analysis software (Phoenix Flow Systems, San Diego, CA, USA) was employed for fitting analysis.

Migration assays

Wound-healing assay

The hDPSCs were plated on solid media in Petri dishes and grown for at least 12 h after transfection. A sterile blue pipette was scored across the center of the cell monolayer to create a wound. The cell surface was rinsed twice to remove detached cells. A phasecontrast microscope equipped with a digital camera (Olympus IX71, Nagano, Japan, 500 µm) was used to capture images of the wounds at the indicated times. The mean distance between the wound margins was determined in several randomly selected fields, directly on photographs, to determine the wound width. The extent of migration was determined by calculating the wound area at time points t0 (time of wounding), t24 (24 h post-wounding) t48 (48 h post-wounding), and t72 (72 h post-wounding). The formula [area (t0) – area (t24 or t48 or t72)]/area(t0)×100% was used for normalization. $p < 0.05$ was considered significant.

Transwell assay

Transfected HEK293T cells were seeded onto the lower layer of 24-well Transwell inserts, and then hDPSCs were co-cultured by seeding 1×10^5 cells/ml in 200 µl of cell suspension onto the upper layer. After 48 h of incubation, the Transwell culture chamber was taken out and lightly washed twice with PBS. The cells were then fixed with 4% paraformaldehyde (PFA) for 30 min, stained with 0.1% crystal violet for 1 h, and washed three times with double-distilled water. Neutral gum was used to seal the slides. Photographs were taken and cell counting were performed under an inverted microscope at high power (Olympus IX71, Nagano, Japan, 100 µm). Five fields were randomly selected for photography and counting of migrated cells.

Odontogenic differentiation

Alizarin red staining

The hDPSCs were transfected, followed by plating on 12-well plates at a density of 5×10^4per well and culturing for 21 d. Thereafter, the hDPSCs were fixed in 4% PFA for 30 min and then rinsed with PBS. Next, the cells were stained with alizarin red solution (pH 4.0-4.2) for 10 min under dark conditions. The stained hDPSCs were then decolored, air-dried, and evaluated using light microscopy under an inverted microscope (Olympus IX71, Nagano, Japan, 200 µm). Image Pro Plus 6.0 software (National Institutes of Health, Bethesda, MD, USA) was used to analyze the staining intensity of the cells in each image [13]. Image pro plus 6.0 software was used to select "Per Area (Obj./Total)" in the measurement method, collect the designated dyeing area, and calculate the result. The staining intensity was directly correlated to the odontoblastic activity of the hDPSCs.

Alkaline phosphatase (ALP) assay

Transfected hDPSCs were seeded in a 12-well plate at a density of 5×10^4per well and cultured for 7 and 14 days, respectively. Thereafter, the hDPSCs were stained with 200 µl of 0.2% lysis buffer solution containing 10 µl Triton X-100 in 5 ml $MgCl_2$, according to the protocol outlined in the ALP analysis kit (DGKC, Pars Azmun, Iran). Photographs of the stained cells on the 12-well plates were taken under an inverted microscope (Olympus IX71, Nagano, Japan, 200 µm). Image pro plus 6.0 software was used to select "Per Area (Obj./Total)" in the measurement method, collect the designated dyeing area, and calculate the result.

RNA sequencing (RNA-seq)

hDPSCs transfected with Wt *EDA1* and its variants were seeded in a 6-well plate at a density of 2×10^5 per well and cultured for 48 h ($n = 3$, three samples per group). The samples were dispatched to iGeneTech Bioscience Co., Ltd. (Beijing, China) for RNA sequencing. An ABclonal mRNA-seq Lib Prep Kit (ABclonal, Wuhan, China) was employed to prepare pairedend libraries according to the supplier's protocol. The AMPure XP system (Beckman Coulter, Indianapolis, IN, USA) was used to purify the PCR products and an Agilent Bioanalyzer 4150 system (Agilent, Santa Clara, CA, USA) was employed to assess

Table 1 Primers used for polymerase chain reaction amplification

genes	Forward (5′-3′)	Reverse (5′-3′)
DMP-1	AAGAGGCCAACCTGTCATCTCA	GGATTCGCTGTCTGCTTGCT
FOS	CTTCCCAGAAGAGATGTCTGTG	TGGGAACAGGAAGTCATCAAAG
FOSB	TCCACACCAGGCATGAGTGG	TCCTTTTGGAGCTCGGCGAT
JUN	GTGCCGAAAAAGGAAGCTGG	CTGTAGCATGAGTTGGC
JUNB	GACCCCTACCGGAGTCTCAA	CTTCCCAGAAGAGATGTCTGTG
GADPH	AAGAGGCCAACCTGTCATCTCA	GGATTCGCTGTCTGCTTGCT

the quality of the library. Ultimately, an Illumina Novaseq 6000 instrument (Illumina, San Diego, CA, USA) or MGISEQ-T7 instrument (MGI, Shenzhen, China) were employed to generate 150 bp paired-end reads. The Illumina or MGI platform data were subjected to bioinformatic analysis. The analyses were performed using an inhouse bioinformatics pipeline from Shanghai Applied Protein Technology (Shanghai, China). DESeq2 (http://bioconductor.org/packages/release/bioc/html/DE Seq2.html) was then used for differential gene expression analysis. In the analysis,| log 2 fold change (FC)| > 1 and an adjusted p-value (Padj) < 0.05 were used as the parameters to identify differentially expressed genes (DEGs).

Quantitative real-time reverse transcription PCR (qRT-PCR)

hDPSCs transfected with *EDA1* variants were treated with TRIzol™ (Thermo Fisher Scientific, Waltham, MA, USA) to extract total RNA, following a standardized protocol for RNA isolation. The Moloney Murine Leukemia Virus Reverse Transcriptase system (Promega GmbH, Mannheim, Germany) was employed to synthesize cDNA from the total RNA following the supplier's guidelines. The cDNA was used as the template in the quantitative realtime PCR (qPCR) step of the qRT-PCR protocol, carried out employing the Applied Biosystems™ 7500 Fast Real-Time PCR System (Thermo Fisher Scientific). The thermal cycling conditions used are available upon request. Normalization of the qPCR data used the glyceraldehyde-3-phosphate dehydrogenase (GAPDH) gene as the housekeeping gene. All determinations were carried out in quintuplicate and the means were derived. The delta-delta Ct method was used to calculate the relative mRNA expression levels.

Statistical processing

The every experiment was repeated for 3 times. The obtained data were statistically analyzed using SPSS26.0 software. Statistical analyses were performed using One-way ANOVA with $p < 0.05$ considered statistically significant.

Results

Wild-type *EDA1* promotes hDPSCs DNA replication in the S phase, thereby enhancing cell proliferation, while *EDA1* variants have lost this ability

In this study, cell proliferation of hDPSCs was assessed using CCK-8 assays (Fig. 1A). Wt-*EDA1* significantly promoted hDPSCs proliferation at all observation time points, compared with that in the NAST-*EDA1* (A259E, S374R) and STA-*EDA1* (H252L) groups ($p < 0.01$). Cell proliferation was also statistically significantly different between the control group and the Wt-*EDA1* group ($p < 0.05$). However, cell proliferation was not significantly different between the control group and the *EDA1* variants.

Flow cytometry analysis of the cell cycle of hDPSCs transfected with *EDA1* variants showed that the proportion of S-phase hDPSCs was markedly higher in the Wt-*EDA1* group compared with that in all variant groups and the control group ($p < 0.05$). The differences observed between variants and the control group were not significant. The proportion of G0/G1 phase cells decreased in Wt-*EDA1* group, although there was no dramatic difference compared with the control group and all the variants ($p > 0.05$). Similarly, there was almost no difference

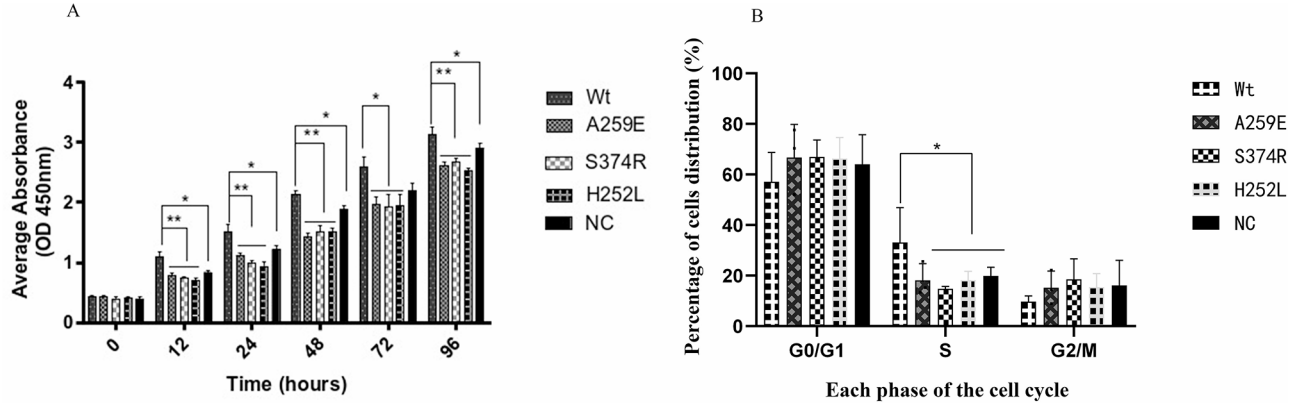

Fig. 1 The influence of *EDA1* on the proliferation and cell cycle distribution of hDPSCs

in the distribution of hDPSCs in the G2/M phase among all the groups ($p > 0.05$) (Table 2; Fig. 1B).

EDA1 variants downregulate the migration of hDPSCs

Wound-healing experiments on hDPSCs expressing Wt *EDA1*and *EDA1* variants (Fig. 2A-B) revealed that the wound area was smallest in the Wt *EDA1* group across all time points. Specifically, at 12 and 24 h post-wounding, the wound area in the Wt group was significantly decreased, indicating an increased migration rate compared with the control group and the syndrome mutation group (H252L) ($p < 0.05$). At 48 and 72 h postwounding, the migration rate of hDPSCs in the variants was decreased compared with that of the Wt group. Indeed, in comparison with the nonsyndromic mutation group (S374R) and the syndrome mutation group (H252L), the wound area of the Wt group was significantly reduced, and the migration rate was significantly increased ($p < 0.05$). At each time point, there was no significant difference in the cell migration rate between variants and the control group.

In the Transwell assay, HEK293T cells transfected with the Wt *EDA1* and variants of *EDA1* were cultured in the lower chamber, while hDPSCs were co-cultured in the upper chamber. The number of hDPSCs passing through the pores was detected at 48 h. It was observed that the highest number of hDPSCs passed through the pore occurred in the wild-type group, with a significant difference compared with that of the variants ($p < 0.05$). The number of migrated hDPSCs in the variant groups was lower than that in the control group, whereas, in the WT *EDA1* group, the number of migrated hDPSCs was higher than that in NC group(Fig. 2C).

Wild-type *EDA1* promotes odontogenic differentiation of hDPSCs

In this study, Alizarin Red staining and ALP staining were used to assess the effect of EDA1 on the mineralization ability of hDPSCs. The results from Alizarin Red staining showed that on the 21st day after the induction of odontogenic differentiation, the overexpression of Wt *EDA1* upregulated the mineralization ability of the hDPSCs. The Wt group showed the highest calcification, while the *EDA1* variants caused reduced calcification in hDPSCs.

Table 2 The influence of *EDA1* mutants on the cell cycle distribution of hDPSCs (mean±SD)

Group	G0/G1 Phase	S Phase	G2/M Phase
Wt	57.17 ± 11.56	33.14 ± 13.74	9.72 ± 2.27
H252L	66.3 ± 8.34	18.21 ± 3.52*	15.49 ± 5.3
A259E	66.7 ± 13.1	18.14 ± 6.57*	15.17 ± 6.66
S374R	66.92 ± 6.71	14.76 ± 0.95*	18.56 ± 8.03
NC	64.06 ± 11.63	19.84 ± 3.45*	16.1 ± 9.94

* indicates *P*<0.5

According to the semi-quantitative analysis of the staining results using Image Pro Plus 6.0, the calcium deposition in both the nonsyndromic and syndromic variants of *EDA1* was dramatically reduced compared with that in the Wt and NC groups ($p < 0.05$). This suggested that the *EDA1* variants inhibit the mineralization of hDPSCs. Additionally, the difference in calcium deposition between the non-syndromic and syndromic *EDA1* mutation groups was not significantly different (Fig. 3A-B).

The results of ALP staining were consistent with those of Alizarine Red staining (Fig. 3C, D). On day 7 and 14 of odontogenic differentiation, the expression of ALP in hDPSCs decreased in the cells expressing the nonsyndromic and syndromic mutants of *EDA1*, whereas expression of Wt *EDA1* promoted ALP expression in hDPSCs. On the 7th day of odontogenic differentiation, compared with that in the Wt and NC groups, ALP expression of ALP was decreased significantly in the nonsyndromic and syndromic mutant groups ($p < 0.05$). On the 14th day of odontogenic differentiation, ALP expression in the non-syndromic and syndromic mutant *EDA1* groups decreased further compared with that in the Wt and NC group ($p < 0.001$). There was no statistically significant difference between the Wt and NC groups. All variants inhibited the expression of ALP in hDPSCs, but there was no statistically difference in ALP expression among the different variants.

We used qRT-PCR to detect the expression level of *DMP1* mRNA (encoding dentin matrix acidic phosphoprotein 1) in hDPSCs during odontogenic differentiation. Compared with that in the Wt group, *DMP1* mRNA expression was significantly downregulated in the *EDA1* variants ($p < 0.05$). However, among the variants, *DMP1* mRNA expression did not differ significantly (Fig. 3E).

RNA sequencing revealed the differential expression of differentially expressed genes (DEGs) and that the *EDA1* variants could not promote *FOS* expression in hDPSCs

The transcriptome data of the all variants were compared with those of the Wt group. Differential gene expression analysis identified common DEGs across each group: *FOS* (encoding Fos proto-oncogene, AP-1 transcription factor subunit), *FOSB* (encoding FosB proto-oncogene, AP-1 transcription factor subunit), *JUN* (encoding Jun proto-oncogene, AP-1 transcription factor subunit), and *JUNB* (encoding JunB protooncogene, AP-1 transcription factor subunit) (Fig. 4A). The data were visualized using a volcano plot, which showed that, compared with the those in the NSTA-S374R group, the expression levels of *FOSB* and *FOS* in the Wt group were significantly increased ($p < 0.05$). Similarly, compared with those in the STA-H252L group, there was markedly increased expression of *FOSB*, *FOS*, and *JUN* in the Wt group ($p < 0.05$)

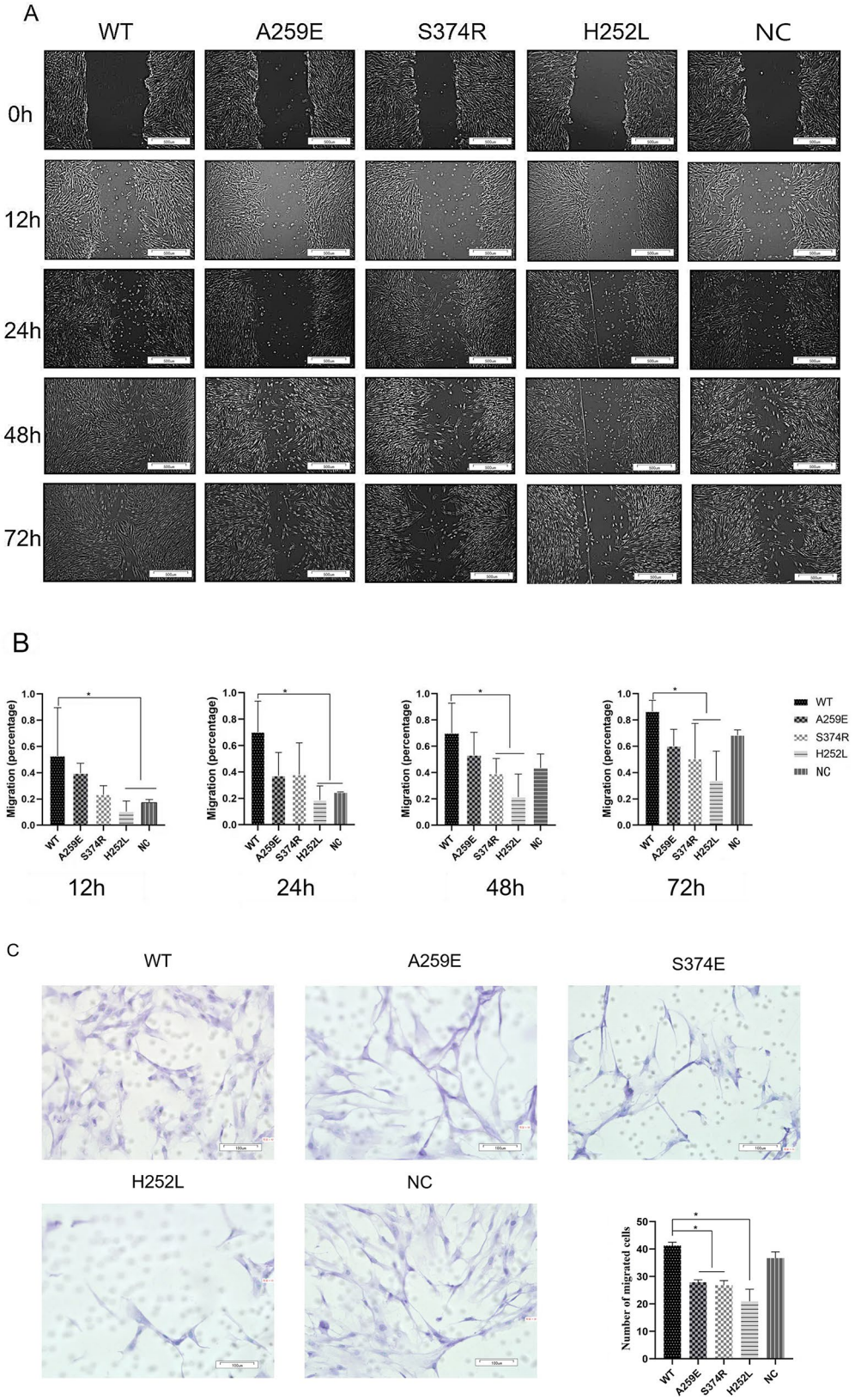

Fig. 2 Effect of *EDA1* variants on the migration of hDPSCs

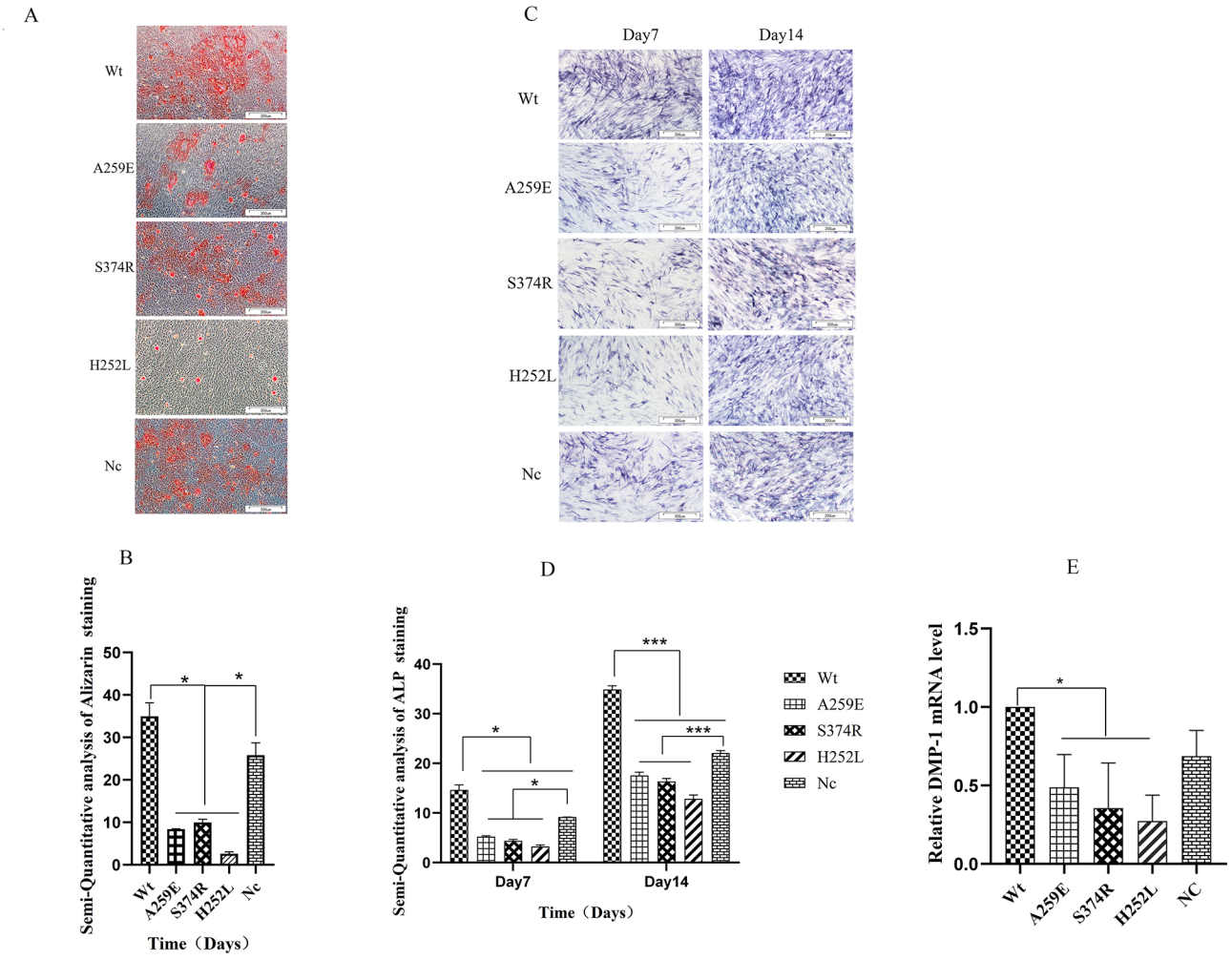

Fig. 3 Effect of *EDA1* on hDPSCs odontogenic differentiation

(Fig. 4A, B). The key hub genes identified were *FOS*, *FOSB*, *JUN*, and *JUNB* (Fig. 4C).

The expression levels of the DEGs (*FOS*, *FOSB*, *JUN*, and *JUNB*) were verified using qRT-PCR. Compared with that in Wt-*EDA1* group, the expression of *FOS* mRNA in the NSTA-*EDA1*, STA-*EDA1* and NC groups decreased significantly ($p < 0.05$). However, there was no significant difference in *FOS* expression between the NC group and the *EDA1* variants. Compared with that in the Wt-*EDA1* group, only the STA*EDA1* group showed a significant decrease in *FOSB* expression ($p < 0.05$), with no difference observed compared with that in the NC group. The results for *JUN* mRNA expression were consistent with those for *FOSB* mRNA. Compared with that in the Wt-*EDA1* group, only the STA*EDA1* and NSTA-*EDA1 (*S374R) group showed a significant decrease in *JUNB* expression ($p < 0.05$) (Fig. 4D). Through qRT-PCR analysis, it was found that only the expression of *FOS* were consistent with the results of RNA-seq, which was statistically significant, the expressions of *FOSB*, *JUN* and *JUNB* was decreased, and only the changes of group H252L were statistically significant($p < 0.05$).

Discussion

Tooth development is regulated by intricate interactions among cells, tissues, and genetic networks. At all tooth developmental stages, the same signaling pathways are active, especially those in ectodermal organs. Pathways such as Wnt/β-catenin, transforming growth factor beta (TGF-β)/bone morphogenetic protein (BMP), Sonic Hedgehog signaling molecule (SHH), and EDA/EDAR/NF-κB interact in a complex regulatory network, playing key roles in regulating the development of embryonic dental structures [14–15]. Disturbances in the homeostasis of these signaling molecules during development can change the number and morphology of teeth [1, 16]. The EDA signaling pathway has a vital function in tooth and skin appendage development [17].

Overexpression of EDA1 increases the placode size [6], whereas a lack of EDA/EDAR signaling results in

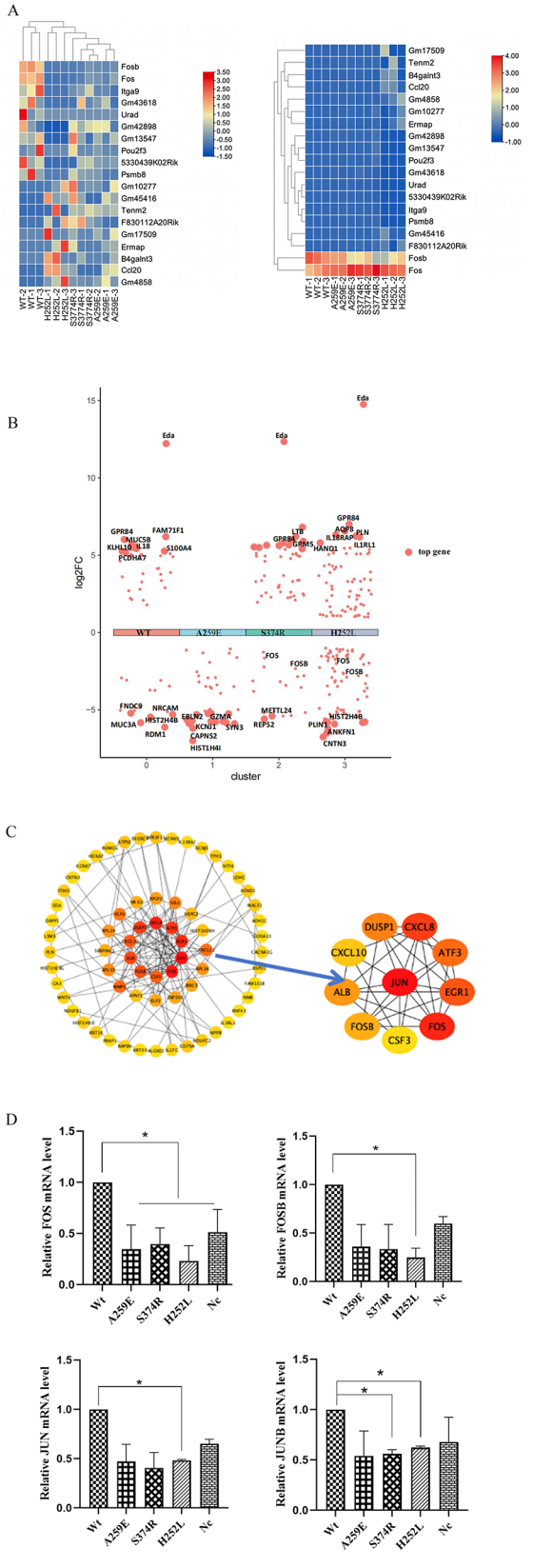

Fig. 4 Analysis of the RNA-seq data and qPCR verification

the formation of a rudimentary pre-placode [18]. Interestingly, *Eda1*-overexpressing mice show induction of ectopic teeth and mammary placodes, and consequently supernumerary organs [6, 19]. These studies show that *EDA1* determines the number of teeth and their morphological development. However, how *EDA1* regulates the epithelial-mesenchymal signaling network to determine the fate of tooth development remains unknown.

The initial morphological clue regarding embryonic dental development is a localized thickening in the surface epithelium. This thickening subsequently invaginates into the underlying mesenchyme, forming a placode. During early morphogenesis, EDA/EDAR signaling regulates the function of the epithelial signaling centers, which are associated with epithelial-mesenchymal interactions. The expression of EDA1 was observed in the dental epithelium of mice at 12 days after the initiation of embryonic development. By day 14, EDA1 expression became localized in the cervical region of developing cap teeth within the oral epithelium and the outer enamel epithelium. Transfection of *EDA1* variants into human umbilical vein endothelial cells showed that the proliferative activity of the cells expressing the variants was significantly decreased. Previously, our research group found that overexpression of *EDA1* in ameloblastoid cell lines in vitro promoted the transformation of G0/G1 phase cells into S phase cells, resulting in cell proliferation, while the syndromic mutant of *EDA1* had lost its ability to promote cell proliferation [20]. It was speculated that a loss of binding of the syndromic variant of *EDA1* to its specific receptor leads to reduced transcription activity of NF-κB in the downstream signaling pathway [5]. This resulted in loss of its ability to induce site-specific proliferation of odontogenic epithelial cells, potentially affecting site-specific development of embryonic teeth. In vivo, in the absence of EDAR/NF-κB signaling, placodes in downless and Tabby mutant mice start to develop, but rapidly abort. Moreover, EDA has a crucial function in promoting the differentiation of bone marrow mesenchymal stem cells (BM-MSCs) into sweat glands. In addition, the expression levels of downstream genes of NF-κB [*SHH* and *CCND1* (encoding cyclin D1)] were also enhanced [21].

In humans, embryonic EDA1 expression occurs in ectodermal tissues and the developing neuroectoderm, thymus, and bone. The expression of EDA/EDAR in sweat glands, teeth, and hair follicles, occurs not only in the epidermis, but also in adjacent dermal mesenchymal cells. However, studies on the effect of EDA1 on the dental mesenchyme are few and thus this aspect requires further investigation. In the present study, we found that wild-type *EDA1* promoted DNA replication in the S phase of the hDPSCs cell cycle, thereby promoting cell proliferation. In contrast, the *EDA1* variants had lost

their ability to promote hDPSCs proliferation, consistent with the effect of *EDA1* on odontogenic epithelial proliferation. It has been suggested that *EDA1* variants lead to a decrease in NF-κB activity in the tooth germ epithelium and mesenchymal cells, which reduces the proliferation activity of dental epithelial and mesenchymal cells, thus affecting the development of the tooth germ [5]. Moreover, we found that *EDA1* plays an important role in the migration of dental pulp stem cells. Overexpression of *EDA1* upregulated the migration of hDPSCs, while overexpression of the nonsyndromic and syndromic variants of *EDA1* downregulated cell migration in vitro. This finding aligns with Iida's evidence that in medaka, EDAR-expressing cells migrate toward elongation of the fin ray, which stimulates mesenchymal proliferation. This is followed by condensation of the mesenchyme and the differentiation of mesenchymal cells into osteoprogenitor cells in the proximal region. In the all-fin less (afl) mutant larvae, fin ray formation onset is characterized by EDAR expression in epithelial cells. However, there is no NF-κB activation because of the loss of binding of EDA to EDAR. Consequently, EDARexpressing cells cannot migrate and remain at the starting point. This restriction leads to mesenchymal condensation and differentiation into osteoprogenitor cells, resulting in the formation of short and thin fin rays [8].

In this study, variants of *EDA1* inhibited ALP activity and the formation of calcified nodules, thereby reducing the ability of hDPSCs to differentiate into dentin in vitro. This reduction might be related to the small tooth morphology, although the underlining mechanism requires further investigation. Additionally, in Tabby mice, epiphyseal and subepiphyseal dysplasia were linked to spontaneous fractures of tail vertebrae [32]. The authors found that in comparison with wild-type calvariae in vivo or osteoclasts in vitro, Tabby calvarial bone and Tabby bone marrow-derived osteoclasts showed significantly reduced activity of osteoclastic co-enzymes, such as cathepsin K, matrix metalloproteinase 9 (MMP9), tartrate-resistant acid phosphatase (TRAP), and T cell immune regulator 1, ATPase H + transporting V0 subunit A3 (TCIRG1). This reduction indicated reduced levels of nuclear factor of activated T cells 1 (Nfatc1) and boneresorbing enzymes, which are likely to underly the osteopetrosis-like changes observed in EDA1-deficient murine calvariae [22]. Taken together, these studies suggest that EDA1 regulates the osteogenic differentiation of dentin and bone. EDA1 binds to its specific receptor EDAR, ultimately activating NF-κB, which is an important regulator of osteoclastic differentiation and skeletal development [23]. The receptor activator of nuclear factor Kappa B ligand (RANKL)-receptor activator of nuclear factor Kappa (RANK)-TNF receptor associated factor 6 (TRAF6) complex is required for NF-κB activation. Disruption of this signaling axis in Tabby mice could interfere with the interactions among EDA1, TRAF6, and RANK, resulting in inhibition of osteoclastic differentiation [24].

Osteoclasts express EDAR [7] and NF-κB has a vital function in osteoclast maturation [25]. Very small amounts of RANKL can synergize with TNF, thereby promoting osteoclastogenesis; therefore, it is plausible that EDA1 might also synergize with RANKL, a hypothesis that warrants further investigation. During the differentiation of osteoclasts, the binding between RANKL and RANK induces or activates the expression of important transcription factors, including purine rich box-1 (PU1), microphthalmia-associated transcription factor (Mitf), cellular oncogene fos (cFos), Nfatc1, and NF-κB, which are all essential for osteoclastogenesis, both in vitro and in vivo [26].

Genome-wide RNA expression profiling of whole skin from adult mice and embryos identified numerous *EDA* target genes [27]. A complementary study profiled the patterns of gene expression in cultured primary keratinocytes obtained from Wt and Tabby mice using a microarray, revealing several candidate target genes of *EDA*, such as *Tbx1* (encoding T-box transcription factor 1), *Bmp7* (encoding bone morphogenetic protein 7), and *Jag1* (encoding jagged canonical notch ligand 1) [28].

During tooth development, various genes, transcription factors, and signal transduction molecules can interact with each other through numerous signaling pathways such as WNT, TNF, and NF-κB. *EDA1* activates NF-κB transcription through the EDANF-κB signaling pathway. NF-κB enters the nucleus to regulate downstream target genes, thereby influencing the proliferation, migration, and mineralization of tooth germ cells. Identifying the specific genes regulated by NF-κB after its nuclear entry, and how they affect tooth germ development, remains a significant focus in dental development research. In this study, hDPSCs were transfected with plasmids encoding variants of nonsydromic *EDA1*, syndromic *EDA1* and wild-type *EDA1*. Consistent with previous studies, our findings showed that cell proliferation and osteogenic differentiation were inhibited in the cells expressing the variants, indicating that wildtype *EDA1* promotes cell proliferation, migration, osteoclast differentiation, and other biological behaviors. In the research on the osteogenic differentiation ability of human dental pulp stem cells using some novel regenerative materials, such as tideglusibdoped nanoparticles(TDg-NPs), silk fibroin coated with reduced graphene oxide(SF/rGO), etc., it was found that TDg-NPs can stimulate the osteogenic differentiation of human dental pulp stem cells by activating the WNT and MPAK pathways, and the expressions of genes such as *DSPP*, *RUNX2*, and *ALP* significantly increased. [29–30]. Consistent with the research on odontogenic differentiation in this article, It

provides a basis for the subsequent research on the regulation of the osteogenic differentiation pathway of human dental pulp stem cells.

Hub genes such as *FOS*, *FOSB*, *JUN*, and *JUNB* were identified by RNA-seq and verified using qRT-PCR. The results revealed that the syndromic *EDA1* variant significantly reduced the transcription levels of activator protein 1 (AP-1) subunits in hDPSCs. Interestingly, the non-syndromic *EDA1* variants primarily affected the transcription level of *FOS*. Therefore, we speculated that different downstream signaling molecules are activated by the *EDA1* variants. The syndromic variant not only affects tooth development, but also impacts the development of other organs, including bone structures, whereas the nonsydromic variant only affects tooth development.

The proteins of the AP-1 family are involved in the regulation of cell proliferation, apoptosis, differentiation, inflammation, immune response, and other physiological and disease-related functions [31]. Studies have demonstrated that AP-1 family members are expressed during various stages of tooth development and play a role in regulating the expression of tooth development-related proteins, such as dentin sialophosphoprotein (DSPP), DMP1, and Amelotin [32–34]. c-Fos is a major subunit of the AP-1 transcription factor complex, which also includes Jun family members. c-Fos has been proposed to be important for cell differentiation, cell proliferation, and signal transduction. In mice, the developing central nervous system, germ cells, hematopoietic cells, teeth, and bones, *c-Fos* is stably expressed. Mice and rats with homozygous *Fos* knock out (KO) are all toothless, indicating that *c-Fos* is crucial for the occurrence and development of tooth germs [35]. In addition, homozygous *Fos* KO rats show abnormal bone development because of a lack of osteoclasts, similar to the situation in in *Fos* KO mice. Thus, *c-Fos* is essential to induce osteoclast differentiation from progenitor cells. As early as 1998, studies cloned the promoter of the mouse *Dspp* gene and identified binding sites for some common transcription factors, including *AP-1*, *AP-2*, *MSX1*, serum response element and *TCF-1*, indicating that *AP-1* may play a role in regulating *Dspp* gene expression. Pang et al. successfully cloned the promoter sequence of the human dentin matric protein 1 (*DMP1*) gene and identified an AP-1 binding site. They found that the − 505 bp to + 86 bp fragment has the strongest activity in hDPSCs [36]. Another study showed that co-expression of *c-Jun* and *c-Fos*, following transfection into MC3T3 cells with a *DMP1* promoter reporter gene vector, increased promoter activity by 1.7 fold, as measured using luciferase assays [37].

Enamel and dentin are part of human mineralization, similar to bone. Patients with X-linked hypohidrotic ectodermal dysplasia (XLHED) and Tabby mice exhibit smaller sized teeth, abnormal cusp morphology, and other mineralization abnormalities. In the present study, Alizarin Red staining revealed that *EDA1* regulates the odontogenic differentiation of dental pulp stem cells in vitro. The variants of *EDA1* induced a reduction in mineralized nodules by hDPSCs, particularly the syndromic *EDA1* variants. However, the mechanism by which *EDA1* affects tooth mineralization remains unclear. RNA sequencing revealed differential expression of AP-1, and further qRT-PCR verification showed that the variants of *EDA1* could not promote the expression of *FOS* mRNA in hDPSCs.

Therefore, we speculated that the variants of *EDA1* fail to promote the expression of *FOS* mRNA in hDPSCs, leading to reduced odontogenic differentiation and proliferation of hDPSCs, thereby affecting tooth development. In the future, our research will focus on uncovering the interaction mechanisms between *EDA1* and other key signaling pathways involved in tooth development, with the goal of identifying new therapeutic targets for gene therapy. As important transcription factors in the body, AP-1 and NF-κB are both activated in response to external stimuli and then exert their functions. Although their regulatory mechanisms are different, studies have found that they can be simultaneously activated by the same multiple stimuli. For instance, the activation of JNK caused by inflammatory factors or stress is often accompanied by the nuclear translocation of NF-κB, and the receptor activator of NF-κB can activate both the transcription factor NF-κB and AP-1. Therefore, there may be some mutual regulatory relationship between them, providing certain research ideas for the subsequent study of the pathway crosstalk mechanism by our research group.

Abbreviations

TA	Tooth Agenesis
EDA1	Ectodysplasin A1
NSTA	Non-Syndromic Tooth Agenesis
STA	Syndromic Tooth Agenesis
hDPSCs	Human Dental Pulp Stem Cells
HED	Hypohidrotic Ectodermal Dysplasia
AP-1	Activator Protein 1
DMP1	Dentin Matric Protein 1
cFos	Cellular Oncogene Fos
NF-κB	Nuclear Factor kappa B
TNF	Tumor Necrosis Factor
RANKL	Receptor Activator of Nuclear Factor Kappa B Ligand
TRAF6	TNF Receptor Associated Factor 6
MMP9	Matrix Metalloproteinase 9
TRAP	Tartrate-Resistant Acid Phosphatase
Nfatc1	Nuclear Factor of Activated T cells 1
PU1	Purine Rich Box-1
Mitf	Microphthalmia-Associated Transcription Factor
Tbx1	T-box Transcription Factor 1
Bmp7	Bone Morphogenetic Protein 7
Jag1	Jagged Canonical Notch Ligand 1
DSPP	Dentin Sialophosphoprotein

Acknowledgements
We thank all study participants for their contributions.

Author contributions
YD, GL: Conceptualization, Data Curation, Formal analysis, Methodology, Writing-original draft, Writing-review & editing. YZ, YZ: Investigation, Validation, Writing-review & editing. JM, JZ, YY, BL: Conceptualization, Software, Resources. WL, WS: Data curation, acquisition, Supervision, Writing-review & editing. All author read and approved the final version of the manuscript.

Funding
This work was supported by the Natural Science Foundation of Hebei Province of China (grant number H2022206246).

Data availability
The raw sequence data reported in this paper have been deposited in the Genome Sequence Archive (Genomics, Proteomics & Bioinformatics 2021) in National Genomics Data Center (Nucleic Acids Res 2024), China National Center for Bioinformation / Beijing Institute of Genomics, Chinese Academy of Sciences (GSA-Human:HRA009018) that are publicly accessible at https://ngdc.cncb.ac.cn/ gsa-human.

Declarations

Ethics approval and consent to participate
All the research procedures performed in this study were in accordance with the ethical standards of the institutional and/or national research committee and with the 1964 World Medical Association Declaration of Helsinki and its later amendments.

Consent for publication
Not applicable.

Competing interests
The authors declare no competing interests.

Author details
[1]Department of Prosthodontics, Hebei Key Laboratory of Stomatology/ Hebei Technology Innovation Center of Oral Health, School and Hospital of Stomatology, Hebei Medical University, Shijiazhuang 050017, China
[2]Department of Stomatology, The No. 2 Hospital of Baoding, Baoding 071051, China
[3]Department of Prosthodontics, Stomatological Hospital Hangzhou, Hangzhou 310000, China
[4]Cancer Genetics & Epigenetics, City of Hope National Medical Center, Duarte, CA 91010, USA
[5]Hebei Eye Hospital, Xingtai 054001, China
[6]Hebei Key Laboratory of Stomatology/ Hebei Technology Innovation Center of Oral Health, School and Hospital of Stomatology, Hebei Medical University, Shijiazhuang 050017, China
[7]Department of Immunology, School of Basic Medicine, Hebei Medical University, Shijiazhuang 050017, China

Received: 11 October 2024 / Accepted: 3 March 2025
Published online: 08 March 2025

References

1. Charles CS, Pantalacci. Effect of eda loss of function on upper jugal tooth morphology. Anat Rec. 2009;292:299–308.
2. Morlon AA, Munnich. Table 2, TRAF6 and TAK1 are involved in NF-kappaB activation induced by the TNF-receptor, Edar and its adaptator Edaradd. Hum Mol Genet. 2005;14:3751–7.
3. Kowalczyk-Quintas CP, Schneider. Ectodysplasin A (EDA) – EDA receptor signalling and its Pharmacological modulation. Cytokine Growth Factor Rev. 2014;25:195–203.
4. Mues GA, Tardivel. Functional analysis of Ectodysplasin-A mutations causing selective tooth agenesis. Eur J Hum Genet. 2010;18:19–25.
5. Shen WY, Wang. Functional study of Ectodysplasin-A mutations causing Non-Syndromic tooth agenesis. PLoS ONE, 2016. 11. e0154884.
6. Mustonen TM, Ilmonen. Ectodysplasin A1 promotes placodal cell fate during early morphogenesis of ectodermal appendages. Dev (Cambridge). 2004;131:4907–19.
7. Kossel CM, Wahlbuhl. Correction of vertebral bone development in Ectodysplasin A1-Deficient mice by prenatal treatment with a replacement protein. Front Genet. 2021;12:1–10.
8. Iida YK, Hibiya. Eda/Edar signaling guides fin ray formation with preceding osteoblast differentiation, as revealed by analyses of the Medaka all-fin less Mutantafl. Dev Dyn. 2014;243:765–77.
9. Cui CM, Durmowicz. EDA targets revealed by skin gene expression profiles of wild-type, Tabby and Tabby EDA-A1 Transgenic mice. Hum Mol Genet. 2002;11:1763–73.
10. Wu XM, Yan. iRoot SP promotes osteo/odontogenesis of bone marrow mesenchymal stem cells via activation of NF-κB and MAPK signaling pathways. Stem Cells Int. 2020;2020:1–15.
11. Wright JTM, Fete. Ectodermal dysplasias: classification and organization by phenotype, genotype and molecular pathway. Am J Med Genet Part A. 2019;179:442–7.
12. Zhang QMJ, Lenardo. 30 Years of NF-kB: A blossomingof relevance to human pathobiology. Cell. 2017;168:37–57.
13. C Jensen E. Quantitative analysis of histological staining and fluorescence using ImageJ. Anat Record (Hoboken N J: 2007). 2013;296:378–81.
14. Yu MSW, Wong. Genetic analysis: Wnt and other pathways in nonsyndromic tooth agenesis. Oral Dis. 2019;25:646–51.
15. Ye XA, Attaie. Genetic basis of nonsyndromic and syndromic tooth agenesis. J Pediatr Genet. 2016;05:198–208.
16. Horakova LL, Dalecka. Eda controls the size of the enamel knot during incisor development. Front Physiol. 2023;13:1–14.
17. Wu ZY, Wang. EDA and EDAR expression at different stages of hair follicle development in cashmere goats and effects on expression of related genes. Archives Anim Breed. 2020;63:461–70.
18. Mou CHA, Thomason. Enhanced ectodysplasin-A receptor (EDAR) signaling alters multiple fiber characteristics to produce the East Asian hair form. Hum Mutat. 2008;29:1405–11.
19. Voutilainen MPH, Lindfors. Ectodysplasin/NF-κB promotes mammary cell fate via Wnt/β-catenin pathway. PLoS Genet, 2015. 11. e1005676.
20. Boyu LK, Xuan-Ting. Effect of A1 protein in ectodermal dysplasia on the proliferation and cell cycle of ameloblastic epithelial cells. Chin J Stomatology. 2019;56:349–54.
21. Sun SJ, Xiao. Targeting Ectodysplasin promotor by CRISPR/dCas9-effector effectively induces the reprogramming of human bone marrow-derived mesenchymal stem cells into sweat gland-like cells. Stem Cell Res Ther. 2018;9:1–10.
22. Schweikl CS, Maier-Wohlfart. Ectodysplasin A1 deficiency leads to Osteopetrosis-like changes in bones of the skull associated with diminished osteoclastic activity. Int J Mol Sci. 2022;23:12189.
23. Smahi AG, Courtois. The NF-κB signalling pathway in human diseases:from incontinentia pigmenti to ectodermal dysplasias and immune-deficiency syndromes. Hum Mol Genet. 2002;11:2371–5.
24. Clauss FMC, Manière. Dento-Craniofacial phenotypes and underlying molecular mechanisms in hypohidrotic ectodermal dysplasia (HED): a review. J Dent Res. 2008;87:1089–99.
25. Asagiri MH, Takayanagi. The molecular Understanding of osteoclast differentiation. Bone. 2007;40:251–64.
26. Teitelbaum SLFP, Ross. Genetic regulation of osteoclast development and function. Nat Rev Genet. 2003;4:638–49.
27. Cui CYT, Hashimoto. Ectodysplasin regulates the lymphotoxin-beta pathway for hair differentiation. Proc Natl Acad Sci U S A. 2006;103:9142–7.
28. Esibizione DC, Cui. Candidate EDA targets revealed by expression profiling of primary keratinocytes from Tabby mutant mice. Gene. 2008;427:42–6.
29. Sergio L-GSD, Aznar-Cervantes. 3D graphene/silk fibroin scaffolds enhance dental pulp stem cell osteo/odontogenic differentiation. Dent Mater. 2023;1:1–10.
30. Osorio RF, J. Mitigating lipopolysaccharide-induced impairment in human dental pulp stem cells with tideglusib-doped nanoparticles: enhancing osteogenic differentiation and mineralization. Dent Mater. 2024;40:1591–601.
31. Ye NY, Ding. Small molecule inhibitors targeting activator protein 1 (AP-1). J Med Chem. 2014;57:6930–48.
32. Xiaona LL, Xianghui. Effects of p38 MAPK Inhibition on the expression of enamel development-related genes in mice. Oral Disease Control. 2021;29:529–34.
33. Lee SYSY, Kim. Effects of Recombinant dentin sialoprotein in dental pulp cells. J Dent Res. 2012;91:407–12.
34. Jianliang PD, Tianzheng. Transcriptional regulation of human dentin matrix protein 1 gene by c-Jun and c-Fos. J Mod Dentistry. 2010;24:443–7.

35. Yoshimura YK, Nakamura. Generation of c-Fos knockout rats, and observation of their phenotype. Exp Anim. 2023;72:95–102.
36. Jianliang PW, Buling. Cloning, sequencing and activity analysis of human dentin matrix protein-1 gene promoter. J Endodontic Periodontology. 2005;15:428–34.
37. Narayanan KA, Ramachandran. Transcriptional regulation of dentin matrix protein 1 (DMP1) by AP-1 (c-fos/c-jun) factors. Connect Tissue Res. 2009;43:365–71.

Publisher's note